THE JOURNAL OF BIOLOGICAL CHEMISTRY
Vol. 278, No. 32, Issue of August 8, pp. 30317–30327, 2003
Printed in U.S.A.

TDAG51 Is Induced by Homocysteine, Promotes Detachment-mediated Programmed Cell Death, and Contributes to the Development of Atherosclerosis in Hyperhomocysteinemia*

Received for publication, December 18, 2002, and in revised form, April 15, 2003
Published, JBC Papers in Press, May 8, 2003, DOI 10.1074/jbc.M212897200

Gazi S. Hossain‡, Johannes V. van Thienen‡, Geoff H. Werstuck‡, Ji Zhou‡, Sudesh K. Sood‡, Jeffrey G. Dickhout‡, A. B. Lawrence de Koning‡, Damu Tang‡, Dongcheng Wu‡, Erling Falk§, Ranjana Poddar¶, Donald W. Jacobsen‖, Kezhong Zhang, Randal J. Kaufman**, and Richard C. Austin‡ ‡‡**

*From the ‡Department of Pathology and Molecular Medicine, McMaster University and the Henderson Research Centre, Hamilton, Ontario L8V 1C3, Canada, the §Department of Cardiology, Aarhus University Hospital, University of Aarhus, Aarhus, Denmark, ¶Boyer Center for Molecular Medicine, Department of Genetics, Yale School of Medicine, New Haven, Connecticut 06536, the ‖Department of Cell Biology, Lerner Research Institute, Cleveland Clinic Foundation, Cleveland, Ohio 44195, and the **Department of Biological Chemistry, Howard Hughes Medical Institute, University of Michigan Medical Center, Ann Arbor, Michigan 48109-0650*

Hyperhomocysteinemia is an independent risk factor for cardiovascular disease and accelerates atherosclerosis in apoE$^{-/-}$ mice. Despite the observations that homocysteine causes endoplasmic reticulum (ER) stress and programmed cell death (PCD) in cultured human vascular endothelial cells, the cellular factors responsible for this effect and their relevance to atherogenesis have not been completely elucidated. We report here that homocysteine induces the expression of T-cell death-associated gene 51 (TDAG51), a member of the pleckstrin homology-related domain family, in cultured human vascular endothelial cells. This effect was observed for other ER stress-inducing agents, including dithiothreitol and tunicamycin. TDAG51 expression was attenuated in homozygous A/A mutant eukaryotic translation initiation factor 2α mouse embryonic fibroblasts treated with homocysteine or tunicamycin, suggesting that ER stress-induced phosphorylation of eukaryotic translation initiation factor 2α is required for TDAG51 transcriptional activation. Transient overexpression of TDAG51 elicited significant changes in cell morphology, decreased cell adhesion, and promoted detachment-mediated PCD. In support of these *in vitro* findings, TDAG51 expression was increased and correlated with PCD in the atherosclerotic lesions from apoE$^{-/-}$ mice fed hyperhomocysteinemic diets, compared with mice fed a control diet. Collectively, these findings provide evidence that TDAG51 is induced by homocysteine, promotes detachment-mediated PCD, and contributes to the development of atherosclerosis observed in hyperhomocysteinemia.

Numerous epidemiological studies have demonstrated that hyperhomocysteinemia is a strong and independent risk factor for cardiovascular disease (1–4). A direct causal relationship between induction of hyperhomocysteinemia and accelerated atherosclerosis has been established in apoE$^{-/-}$ mice fed hyperhomocysteinemic diets (5, 6). These mice showed enhanced vascular inflammation, and atherosclerotic lesion area and complexity. Furthermore, dietary enrichment in vitamin cofactors essential for intracellular homocysteine metabolism attenuated the development of atherosclerosis (5). Although diet-induced hyperhomocysteinemia accelerates early lesion development and enhances plaque fibrosis in apoE$^{-/-}$ mice, no difference in lesion size between control and hyperhomocysteinemic mice was observed after long term treatment (6). These findings imply that hyperhomocysteinemia mediates the early stages of atherogenesis.

Several hypotheses have been proposed to explain the proatherogenic effects of homocysteine. Because the thiol group of homocysteine readily undergoes autoxidation in plasma to generate reactive oxygen species, it has been suggested that homocysteine induces cell injury/dysfunction through a mechanism involving oxidative stress (4, 7). This hypothesis, however, fails to explain why cysteine, which is present in plasma at much higher concentrations than homocysteine and is also readily autoxidized, does not cause cell injury and is not considered a risk factor for cardiovascular disease (8, 9). The observation that homocysteine decreases the expression of a wide range of antioxidant enzymes (10) and inhibits glutathione peroxidase activity (11) raises the possibility that homocysteine may enhance the cytotoxic effect of agents or conditions known to generate reactive oxygen species. Given that homocysteine is generated intracellularly and can accumulate in cells (12), Jacobsen (8) has recently proposed the molecular target hypothesis, which states that homocysteine can interact and modulate the activity of both large (enzymes, receptors) and small molecular (nitric oxide, glutathione) targets, thereby altering specific cellular processes and pathways.

Consistent with the molecular target hypothesis, we (10, 13) and others (14, 15) have reported that homocysteine acts intracellularly to disrupt protein folding in the endoplasmic reticulum (ER),[1] thereby leading to activation of the unfolded protein response

* This work was supported by Heart and Stroke Foundation of Ontario Grant T-4005, Canadian Institutes of Health Research Grant MOP-49417, and a grant from the Ontario Research and Development Challenge Fund (to R. C. A.). This work was also partially supported by National Institutes of Health Grant RO1HL52234 (to D. W. J.). The costs of publication of this article were defrayed in part by the payment of page charges. This article must therefore be hereby marked "*advertisement*" in accordance with 18 U.S.C. Section 1734 solely to indicate this fact.

‡‡ Career Investigator of the Heart and Stroke Foundation of Ontario. To whom correspondence should be addressed: Henderson Research Centre, 711 Concession St., Hamilton, Ontario L8V 1C3, Canada. Tel.: 905-527-2299 (ext. 42628); Fax: 905-575-2646; E-mail: raustin@thrombosis.hhscr.org.

[1] The abbreviations used are: ER, endoplasmic reticulum; PCD, programmed cell death; TDAG51, T-cell death-associated gene 51; eIF2α, eukaryotic translation initiation factor 2α; TUNEL, TdT-mediated dUTP nick end labeling; GFP, green fluorescent protein; UPR, unfolded protein response; HUVEC, human umbilical vein endothelial cell(s); HAEC, human aortic endothelial cell(s); MEF, mouse embryonic fibroblast(s); GFP, green fluorescent protein; PARP, poly(ADP-ribose) polymerase; ZVAD, benzyloxycarbonyl-Val-Ala-Asp.

(UPR) and increased expression of several ER stress response genes, including *GRP78*, *GRP94*, *GADD153*, *Herp*, and *RTP*. Homocysteine-induced ER stress also increases lipid biosynthesis by activating the sterol regulatory element-binding proteins, thereby promoting hepatic steatosis in mice having diet-induced hyperhomocysteinemia (16). Recent studies have now shown that homocysteine induces programmed cell death (PCD) in cultured human vascular endothelial cells and that this effect involves activation of the UPR (17, 18). Furthermore, the activation of caspase-3 was shown to be essential for this process, a result consistent with the ability of homocysteine thiolactone, a cyclic thioester of homocysteine synthesized by specific aminoacyl-tRNA synthetases (12), to induce PCD in HL-60 cells (19). Although these studies provide *in vitro* evidence that homocysteine and its derivatives can promote PCD, further studies are required to identify the proapoptotic factors involved in this process as well as their *in vivo* relevance to the development of atherosclerosis.

In this report, we demonstrate that homocysteine induces the expression of T-cell death-associated gene 51 (TDAG51), a member of the pleckstrin homology-related domain family (20–22). Overexpression of TDAG51 caused changes in cell morphology, decreased cell adhesion, and promoted detachment-mediated PCD in cultured human vascular endothelial cells. In support of these *in vitro* findings, TDAG51 expression and PCD were increased and co-localized in the atherosclerotic lesions from apoE$^{-/-}$ mice having diet-induced hyperhomocysteinemia, compared with control mice. These studies provide novel evidence that TDAG51 is induced by homocysteine, promotes detachment-mediated PCD, and contributes to atherosclerotic lesion development observed in hyperhomocysteinemia.

EXPERIMENTAL PROCEDURES

Cell Culture and Treatment Conditions—Primary human umbilical vein endothelial cells (HUVEC), human aortic endothelial cells (HAEC), and human aortic smooth muscle cells were purchased from Clonetics (San Diego, CA) and cultured in EGM-2 medium (Clonetics) supplemented with 2% fetal bovine serum, 50 μg/ml gentamicin, 50 ng/ml amphotericin, and a mixture of growth factors. Wild-type and homozygous A/A eukaryotic translation initiation factor 2α (eIF2α) mutant mouse embryonic fibroblasts (MEF) derived from 14.5-day embryos were prepared and cultured as described previously (23). DL-Homocysteine, L-homoserine, L-methionine, L-cysteine, L-homocystine, and DL-dithiothreitol (Sigma) were prepared in fresh medium, sterilized by filtration, and added to cell cultures at the indicated concentrations. Cell growth rates and adherence were monitored using a Z Series Coulter Counter. Cell death was assessed by measuring the release of lactate dehydrogenase into the medium using the Cytotoxicity Detection Kit (Roche Diagnostics).

ApoE$^{-/-}$ Mice and Diets—Female apoE$^{-/-}$ mice, back-crossed 9–10 generations onto a C57BL/6 background, were obtained from Transgenic Alliance (Lyon, France) or Jackson Laboratories (Bar Harbor, ME). At 6 weeks of age, mice were divided into control group fed a low fat/vitamin-defined purified diet (Special Diet Services (Witham, UK) or Harlan Teklad (Madison, WI)) or hyperhomocysteinemic groups fed the same diet but supplemented with either 0.09% (w/v) DL-homocysteine in the drinking water or 1.4% (w/w) L-methionine in the diet. Mice were sacrificed after 4 or 18 weeks on the diets.

Plasma Total Homocysteine and Lipids—Upon sacrifice, blood was withdrawn from the right ventricle into chilled EDTA-containing microtubes and centrifuged immediately. Plasma total homocysteine and lipids were measured from plasma as described previously (6).

Atherosclerotic Lesion Analysis—After blood sampling, mice were flushed with ice-cold saline containing St. Thomas cardioplegic solution and heparin, perfusion-fixed (1× PBS containing 4% formaldehyde, pH 7.2), and immersed in fixative overnight. The heart containing the aortic root was removed, embedded in paraffin, and sectioned as described previously (6).

Preparation of Total RNA, mRNA Differential Display, and Northern Blot Analysis—Isolation of total RNA, mRNA differential display, and identification of candidate cDNA fragments were performed as described previously (13). Candidate cDNA fragments were subsequently amplified by PCR and used as probes on Northern blots.

Northern blot analysis was performed as described previously (10, 13). A multiple tissue Northern blot (2 μg of poly(A)$^+$ RNA/lane) was purchased from Clontech Laboratories Inc., (Mississauga, ON). Specific cDNA probes for *TDAG51* and *GRP78* were radiolabeled with [α-^{32}P]dCTP (specific activity >3000 Ci/mM; PerkinElmer Life Sciences) using a random primed DNA labeling kit (Roche Diagnostics). To normalize for differences in RNA loading, blots were hybridized with a human actin or glyceraldehyde-3-phosphate dehydrogenase cDNA probe.

Cloning and Sequencing of cDNA Fragments—cDNA fragments were subcloned into T-ended pBluescript (KS) and sequenced by fluorescence-based double-stranded DNA sequencing (Institute for Molecular Biology (MOBIX), McMaster University). The cDNA sequences were analyzed and compared for similarity with those sequences available in the GenBank™ data base.

cDNA Library Screening—A HUVEC cDNA library in λgt11 (Clontech) was screened using a radiolabeled EC-C3 cDNA probe (Fig. 1). Positive cDNA phage clones were plaque-purified, and the size of the cDNA inserts was determined by PCR using λgt11 forward and reverse primers (MOBIX). The largest cDNA inserts were excised from the λgt11 vector with *Eco*RI and subcloned into the *Eco*RI site of pBluescript II (KS). A HUVEC cDNA library in the bacterial vector pEAK12 (Edge Biosystems, Gaithersburg, MD) was screened with a radiolabeled 6-2 cDNA probe, and positive bacterial colonies were isolated. Plasmid DNA was isolated from 6-2-positive cells using the QIAEX miniprep kit (Qiagen Inc., Mississauga, ON, Canada), and the size of the inserts was determined by restriction analysis using *Not*I and *Hin*dIII. DNA sequencing and homology searches were done as described above.

Construction of TDAG51 Expression Plasmids—The cDNA encoding the open reading frame of human TDAG51 was amplified by PCR using Vent DNA polymerase (New England Biolabs, Mississauga, ON, Canada) and the expressed sequence tag cDNA clone, AI589460 (American Type Culture Collection, Manassas, VA), as a template (Fig. 1). The forward primer AB19652 (5′-CTT AAG CTT CTT ATG CTG GGA GG**A TG**C TG-3′) contained a terminal *Hin*dIII restriction site (underlined) prior to the initiating ATG (boldface type). The reverse primer AB19653 (5′-GAA TTC TAG A**TC A**GG CAG AGT TGG AGG TGC T-3′) contained a terminal *Xba*I restriction site (underlined) adjacent to the termination codon (boldface type). Following PCR, the amplified TDAG51 cDNA was digested with *Hin*dIII and *Xba*I, and cloned in frame into the *Hin*dIII/*Xba*I sites of pEGFP-C1 (Clontech), generating a fusion protein of the mammalian codon-optimized enhanced green fluorescent protein (GFP) with TDAG51 linked to its C terminus (designated GFP-TDAG51). The TDAG51 cDNA was also cloned into the *Hin*dIII/*Xba*I sites of the mammalian expression vector pcDNA3.1(+) (Invitrogen) to express the native TDAG51 protein. Authenticity of these constructs was confirmed by DNA sequencing (MOBIX).

Transient Transfection of Cells—Transient transfections were performed with Superfect Transfection Reagent (Qiagen) according to the manufacturer's protocol. In brief, a routine transfection experiment involved the addition of plasmid DNA/Superfect transfection reagent mixture to cells in medium for 2–3 h, followed by the addition of complete medium for time periods up to 48 h. Cells were fixed in 4% paraformaldehyde and examined for expression of GFP or the GFP-TDAG51 fusion protein by epifluorescence microscopy using a Zeiss Axioskop 2 microscope. Images were captured using a CCD color video camera (Sony; Tokyo, Japan) and image analysis/archival software (Northern Exposure; Empix Inc., Mississauga, ON). Transfection efficiencies of ~30% were routinely obtained.

Subcellular Fractionation—Isolation of nuclear and cytoplasmic fractions was performed using NE-PER™ nuclear and cytoplasmic extraction reagents according to the manufacturer's instructions (Pierce). Cellular fractions were solubilized in SDS-PAGE sample buffer and stored at −20 °C.

Antibodies—Anti-TDAG51 and anti-E2F-1 polyclonal antibodies were purchased from Santa Cruz Biotechnology (Santa Cruz, CA). Anti-catalase polyclonal antibodies were purchased from Calbiochem. Anti-PARP polyclonal antibodies were purchased from Upstate Biotechnology, Inc. (Lake Placid, NY). Anti-KDEL, anti-GFP, anti-membrin, and anti-HSP60 monoclonal antibodies were purchased from StressGen (Victoria, BC, Canada). Anti-caspase-3/CPP32 and anti-focal adhesion kinase monoclonal antibodies were purchased from Transduction Laboratories (Mississauga, ON, Canada). The H4A3 monoclonal antibody was obtained from the University of Iowa.

Immunoblot Analysis—Immunoblot analysis was performed on total cell lysates as described previously (10, 13). Total cellular proteins were solubilized in SDS-PAGE sample buffer, separated on 10% SDS-polyacrylamide gels under reducing conditions, and transferred to nitrocel-

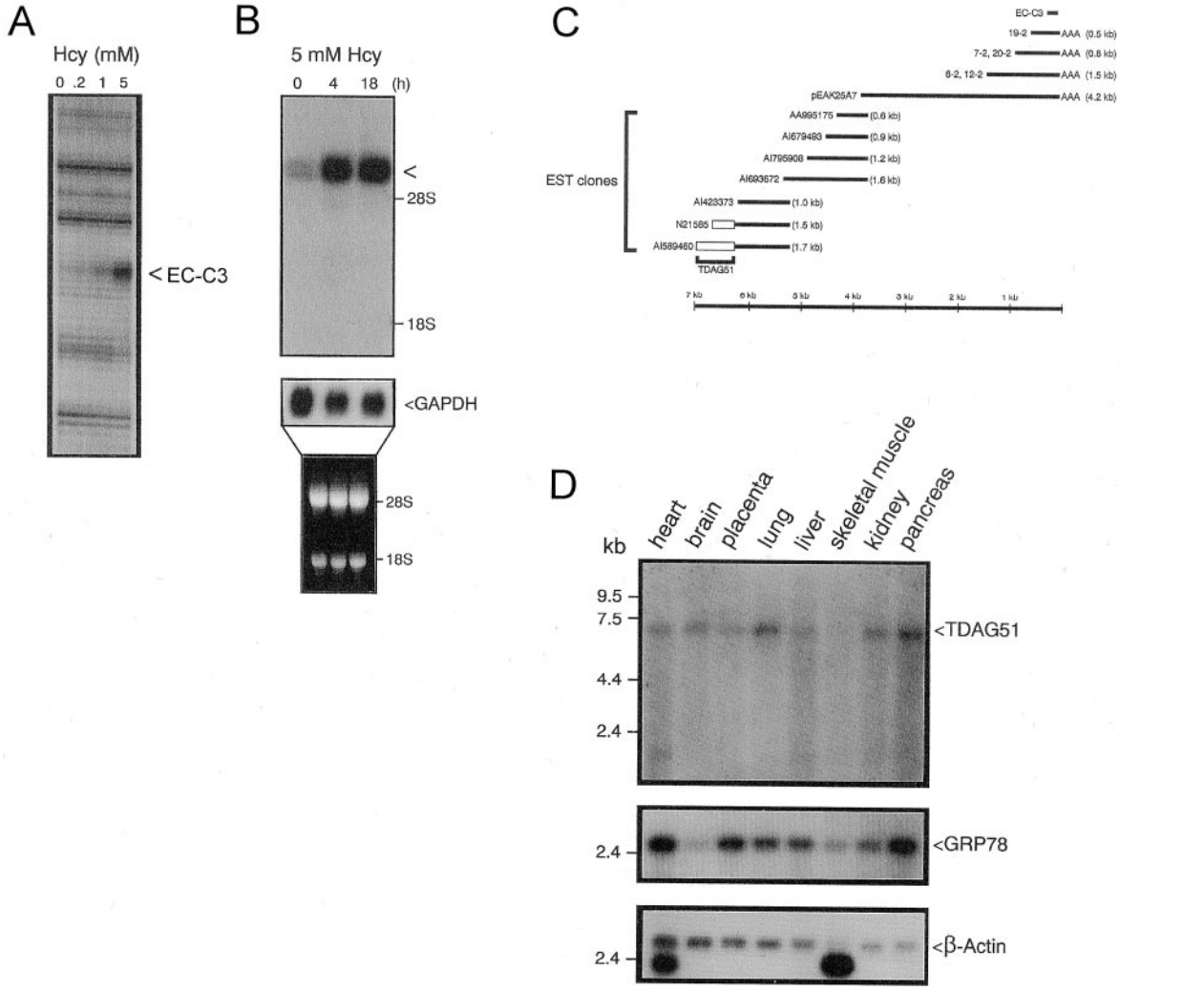

FIG. 1. **Identification of TDAG51 as a homocysteine-inducible gene and its expression in human tissues.** *A*, identification of a homocysteine-inducible gene in HUVEC by mRNA differential display. Total RNA isolated from HUVEC treated for 18 h in the absence or presence of 0.2, 1, or 5 mM homocysteine (*Hcy*) was subjected to mRNA differential display using primers 5′-AAGCT$_{11}$C-3′ and 5′-AAGCTTTGGTCAG-3′. Radiolabeled PCR products were separated on a 6% denaturing sequencing gel and visualized by autoradiography. The arrowhead indicates the position of a cDNA fragment (designated *EC-C3*) that was reproducibly induced by 1 and 5 mM homocysteine. *B*, Northern blot analysis of total RNA (10 μg/lane) from HUVEC treated for 4 or 18 h in the absence or presence of 5 mM homocysteine (*Hcy*) probed with a radiolabeled *EC-C3* cDNA fragment (*upper panel*). The position of the ~7.0-kb mRNA transcript induced by homocysteine is indicated by the *arrowhead*. Control for RNA loading was assessed using a glyceraldehyde-3-phosphate dehydrogenase (*GAPDH*) cDNA probe (*middle panel*) and ethidium bromide staining of the 28 and 18 S rRNA bands (*bottom panel*). *C*, schematic representation of the cloning strategy used to identify and clone *TDAG51*. *EC-C3*, the original homocysteine-induced cDNA fragment identified on differential display gels. *Solid bars*, either cDNA clones obtained from HUVEC library screens or expressed sequence tag clones. The *TDAG51* open reading frame is indicated by the *open rectangle*. *D*, expression of *TDAG51* and *GRP78* in human tissues. A human multiple tissue Northern blot (2 μg of poly(A)$^+$ RNA/lane) was probed with radiolabeled cDNAs specific for *TDAG51* or *GRP78*. Migration positions of standard RNA markers are shown. Hybridization to a *β-actin* cDNA probe was used to normalize RNA loading.

lulose membranes (Bio-Rad). Following incubation with the appropriate primary and horseradish peroxidase-conjugated secondary antibodies (Affinity Biologicals, Hamilton, ON, Canada), membranes were developed using the Renaissance Western blot Chemiluminescence Reagent (PerkinElmer Life Sciences).

Indirect Immunofluorescence—Indirect immunofluorescence was performed on cells and tissues as described previously (10, 16). Primary antibody binding sites were detected using either Alexa^{TM} 488 or Alexa^{TM} 594 donkey anti-goat IgG (Molecular Probes, Inc., Eugene, OR). A Carl Zeiss LSM510 laser-scanning confocal microscope was used to examine immunofluorescently labeled HUVEC and HAEC to localize endogenously expressed TDAG51 and determine its co-localization with catalase, GRP78, membrin, HSP60, H4A3, and/or focal adhesion kinase. Optical sectioning was performed throughout the depth of the cells at 1.5-μm intervals, providing adequate spacial resolution to determine protein localization within regions of the cell and co-localization with other marker proteins.

TdT-mediated dUTP Nick End Labeling (TUNEL) Assay—Cells transiently transfected with the pEGFP-C1 (designated GFP) or pEGFP-C1-TDAG51 (designated GFP-TDAG51) expression plasmids were fixed in 1× PBS containing 4% paraformaldehyde, washed in 1× PBS, and permeabilized with 0.1% Triton X-100. The TUNEL assay was performed using an *in situ* cell death detection kit (Roche Diagnostics). The 3′-nick ends were then labeled by incubating tetramethylrhodamine-dUTP with terminal deoxynucleotidyl transferase. Fixed cells in which terminal deoxynucleotidyl transferase was omitted served as a negative control.

Paraffin-embedded tissue sections were deparaffinized, treated with 0.3% H_2O_2, and washed in 1× PBS. Sections were then incubated with proteinase K (20 μg/ml), washed in 1× PBS, permeabilized with 0.1% Triton X-100, and rinsed with 1× PBS. TUNEL assay was performed as described above, and the 3′-nick ends were labeled by incubating fluorescence-dUTP with terminal deoxynucleotidyltransferase. After TUNEL staining, tissue sections were blocked with 3% bovine serum albumin in 1× PBS, and indirect immunofluorescence for TDAG51 was performed. Sections without primary antibody served as a negative control. After rinsing with 1× PBS, sections were mounted onto coverslips using Prolong Antifade Kit (Molecular Probes, Inc., Eugene, OR).

DNA Fragmentation Assay—HAEC were treated for 24 h in the absence or presence of various concentrations of homocysteine (0.05–10

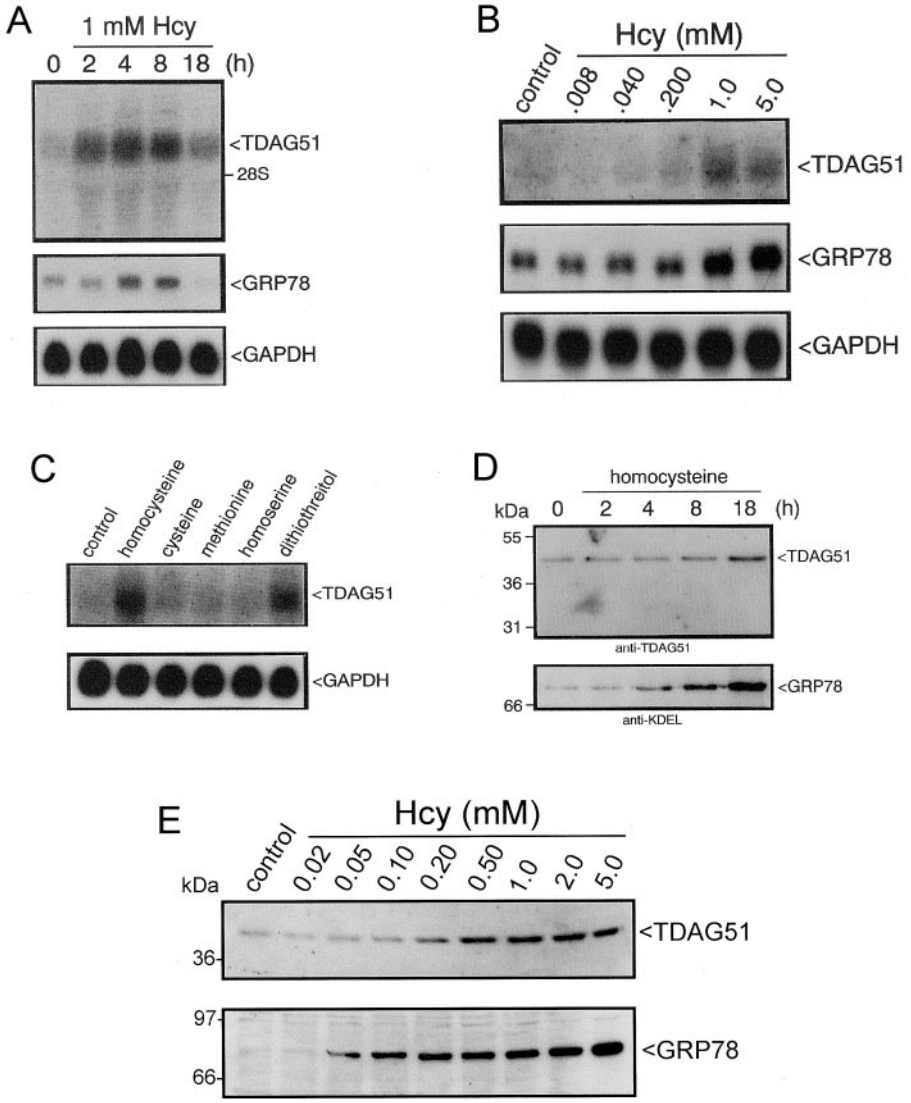

FIG. 2. **Homocysteine induces the expression of *TDAG51* and *GRP78* in vascular endothelial cells.** *A*, time-dependent induction in the steady-state mRNA levels of *TDAG51* and *GRP78*. Total RNA (10 μg/lane) was isolated from HUVEC cultured in the absence or presence of 1 mM homocysteine (*Hcy*) for the indicated time periods. *B*, dose-dependent induction in the steady-state mRNA levels of *TDAG51* and *GRP78*. Total RNA was isolated from HUVEC cultured in the absence (*control*) or presence of increasing concentrations of homocysteine for 4 h. *C*, steady-state mRNA levels of *TDAG51* are induced in HUVEC treated with homocysteine or dithiothreitol. Total RNA (10 μg/lane) isolated from HUVEC cultured for 4 h in the absence (*control*) or presence of 1 mM homocysteine, cysteine, methionine, homoserine, or dithiothreitol. *TDAG51* or *GRP78* mRNA transcripts were detected using radiolabeled cDNA probes, followed by autoradiography. Hybridization to a glyceraldehyde-3-phosphate dehydrogenase (*GAPDH*) cDNA probe was used to normalize RNA loading. *D*, homocysteine increases TDAG51 and GRP78 protein levels in HUVEC. Total protein lysates (40 μg/lane) from HUVEC cultured in the absence or presence of 1 mM homocysteine for the indicated time periods were examined by immunoblot analysis using antibodies to either TDAG51 or GRP78. *E*, homocysteine increases TDAG51 and GRP78 protein levels in HAEC. Total protein lysates (40 μg/lane) from HAEC cultured in the absence (*control*) or presence of increasing concentrations of homocysteine for 18 h were examined by immunoblot analysis.

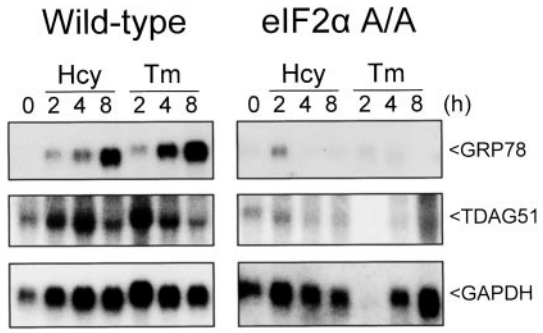

FIG. 3. **eIF2α is required for *TDAG51* expression in response to ER stress.** Northern blot analysis of total RNA from wild type or homozygous A/A mutant eIF2α mouse embryonic fibroblasts treated with 5 mM homocysteine (*Hcy*) or 10 μg/ml tunicamycin (*Tm*) for the indicated time periods. *TDAG51* or *GRP78* mRNA transcripts were detected using the appropriate radiolabeled cDNA probe. Hybridization to a glyceraldehyde-3-phosphate dehydrogenase (*GAPDH*) cDNA probe was used to normalize RNA loading.

mM), 0.5 mM methionine, 0.5 mM cysteine, or 0.5 mM homocystine. The cells (floating and adherent) were harvested by scraping, pelleted, and lysed in 20 mM Tris-HCl, 10 mM EDTA, 0.5% Triton X-100, pH 8.0, on ice for 45 min. The nuclear pellet was collected by centrifugation and resuspended in 0.1 M Tris-HCl, pH 8.5, 5 mM EDTA, 0.2 M NaCl, 0.2% SDS (w/v), and 0.2 mg/ml proteinase K, at 37 °C overnight. NaCl was added to a final concentration of 1.5 M, and the DNA was ethanol-precipitated and resuspended in Tris-EDTA, pH 8.0, containing 200 mg/ml DNase-free RNase A. Following incubation at 37 °C overnight, the DNA was separated on a 2% agarose gel and visualized under UV light after staining with ethidium bromide.

Statistical Analysis—Data are presented as the means ± S.E. Significance of differences between control and treated groups was determined by one-way analysis of variance. If significant differences were detected, unpaired Student's *t* tests were performed. For all analyses, p values <0.05 were considered significant.

RESULTS

TDAG51 Is a Homocysteine-inducible Gene—To identify candidate proapoptotic genes induced by homocysteine, RNA from control or homocysteine-treated HUVEC was subjected to mRNA differential display, as described previously (13). Among a number of differentially expressed cDNA fragments, a 114-bp fragment (designated *EC-C3*) was up-regulated in HUVEC exposed to homocysteine (Fig. 1*A*). Northern blot hybridization experiments using *EC-C3* as a probe identified a homocysteine-inducible transcript of ~7.0 kb in HUVEC (Fig. 1*B*). Although sequence analysis demonstrated that *EC-C3* contained a putative polyadenylation signal (AATAAA), it had no sequence similarity to any known human genes deposited in GenBank™. To obtain larger cDNA clones, HUVEC libraries in λgt11 and in bacteria were screened with *EC-C3*. A number of positive clones were identified and isolated (Fig. 1*C*), with the largest being ~4.2 kb in size (*pEAK25A7*). Although no sequence similarity to any known human genes was observed,

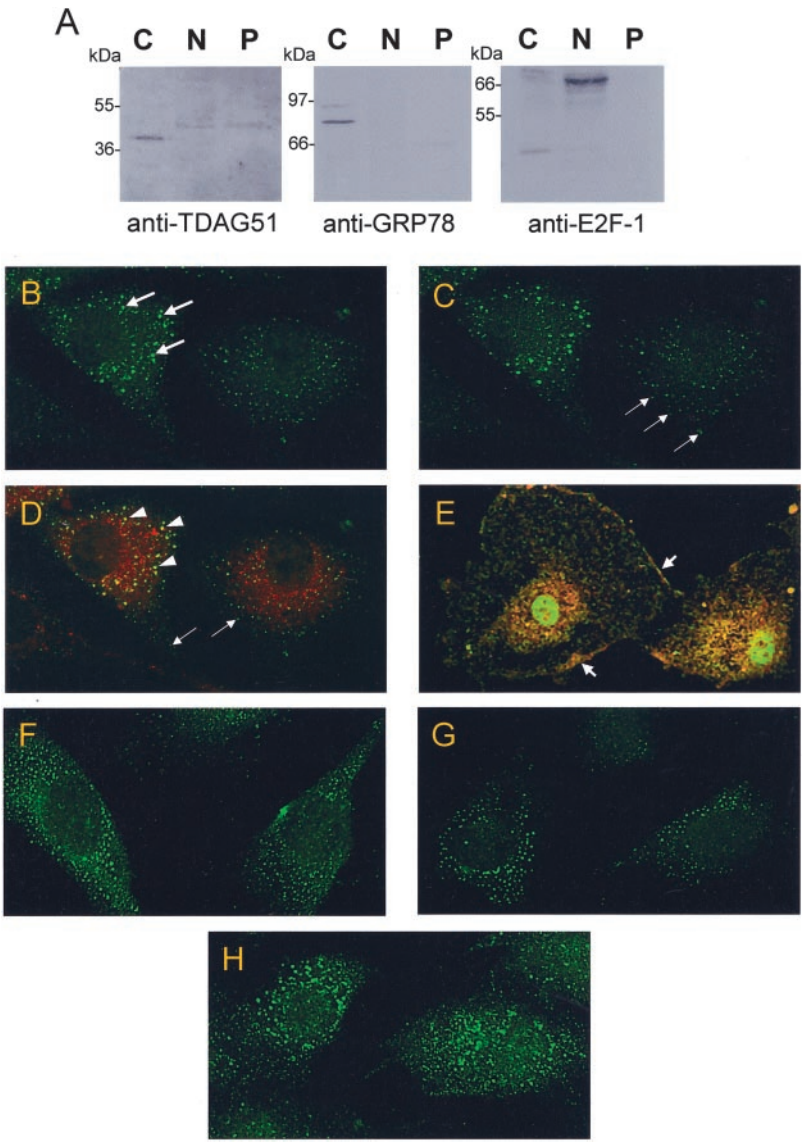

FIG. 4. **Subcellular localization of TDAG51 in vascular endothelial cells.** *A*, nuclear (*N*), cytoplasmic (*C*), and membrane (*P*) fractions isolated from control HUVEC were subjected to immunoblot analysis using anti-TDAG51 antibodies. Purity of the subcellular fractions was confirmed by immunostaining with antibodies specific to cytoplasmic (GRP78) or nuclear (E2F-1) marker proteins. *B–E*, co-localization of TDAG51 with intracellular vesicles. HUVEC grown on gelatin-coated glass coverslips were fixed, permeabilized, and immunostained with antibodies to TDAG51, catalase, or focal adhesion kinase. Cells were optically sectioned throughout their depth at 1.5-μm intervals using laser-scanning confocal microscopy. Endogenously expressed TDAG51 protein was found to be associated with cytoplasmic vesicles of two types: large vesicles found predominately in the perinuclear region centrally located in the depth of the cell (*B*, *large arrows*) and smaller vesicles that were adjacent to the cytoplasmic membrane at the periphery of the cell (*C*, *small arrows*). *D*, TDAG51 (*green*) in the larger perinuclear vesicles co-localized (*yellow regions*) with catalase (*red*), a peroxisome marker (*large arrowheads*). TDAG51 associated with the smaller vesicles did not co-localize with catalase (*D*, *small arrows*). *E*, the small cytoplasmic vesicles of TDAG51 (*red*) co-localized with focal adhesion kinase (*green*) at the cell membrane periphery (*arrows*). *F–H*, effect of homocysteine on the cellular distribution of TDAG51. HUVEC were treated in the absence (*F*) or presence of 1 mM homocysteine for 30 min (*G*) or 24 h (*H*). Original magnification was ×630.

the 5′-end of *pEAK25A7* showed significant sequence similarity to the 3′ end of several human expressed sequence tag clones (GenBank™ accession numbers AA995175, AI679493, AI795908, and AI693672). Identification of additional 5′ expressed sequence tag clones (GenBank™ accession numbers N21585 and AI589460) revealed homology to an open reading frame encoding TDAG51, a member of the pleckstrin homology-related domain family having proapoptotic characteristics (20–22). Furthermore, the size of the *TDAG51* mRNA transcript observed here (~7.0 kb) is consistent with that reported for *TDAG51* transcripts in adult human brain (24).

To further examine the effect of homocysteine on *TDAG51* expression, Northern blot analysis was performed and revealed that the steady-state mRNA levels of *TDAG51* were increased in HUVEC by homocysteine in both a time-dependent (Fig. 2*A*) and concentration-dependent (Fig. 2*B*) manner and correlated with an increase in the steady-state mRNA levels of *GRP78*, an ER-resident molecular chaperone responsive to ER stress. This effect was specific for homocysteine, because other structurally similar amino acids such as methionine, cysteine, and homoserine failed to induce *TDAG51* expression (Fig. 2*C*). The ability of other ER stress agents such as tunicamycin and dithiothreitol (Fig. 2*C*) to increase the expression of *TDAG51* supports a mechanism involving ER stress and UPR activation. This effect of homocysteine did not involve oxidative stress, because (i) the addition of catalase to the cell culture medium failed to inhibit *TDAG51* expression in the presence of homocysteine, and (ii) hydrogen peroxide did not induce the expression of *TDAG51* in HUVEC (data not shown).

To determine whether the increase in the steady-state mRNA levels of *TDAG51* corresponded to an increase in TDAG51 protein, HUVEC were cultured in the absence or presence of homocysteine, and total cell lysates were examined by immunoblot analysis using a polyclonal antibody directed against TDAG51 (Fig. 2*D*). TDAG51 protein was increased in HUVEC following exposure to homocysteine and correlated with an increase in GRP78 protein. Consistent with these findings, TDAG51 and GRP78 proteins were increased in HAEC in a dose-dependent (50 μM to 5 mM) manner following treatment with increasing concentrations of homocysteine for 18 h (Fig. 2*E*). The observation that TDAG51 and GRP78 protein levels were increased at physiological concentrations of 50–200 μM homocysteine suggests that HAEC are more sensitive to exogenous levels of homocysteine then are HUVEC (10, 13).

Recent studies have demonstrated that UPR activation of PERK causes phosphorylation of eIF2α, which is required for the inhibition of cellular mRNA translation and transcriptional induction of the majority of ER stress response genes, including *GRP78*, *GRP94*, and *GADD153* (23, 25). To provide insight into

whether *TDAG51* expression is mediated by eIF2α phosphorylation, we assessed the steady-state mRNA levels of *TDAG51* upon activation of ER stress by homocysteine or tunicamycin in wild-type and homozygous A/A eIF2α mutant MEF (Fig. 3). Whereas homocysteine and tunicamycin induced steady-state mRNA levels of both *TDAG51* and *GRP78* in wild-type MEF, induction was attenuated in the homozygous mutant MEFs. These findings provide evidence that *TDAG51* transcriptional activation is dependent on eIF2α phosphorylation and that *TDAG51* can be classified as an ER stress response gene.

Tissue Distribution of TDAG51—To determine the tissue distribution of TDAG51 expression, Northern blot analysis was performed on poly(A)$^+$ RNA from various human tissues using a radiolabeled TDAG51-specific cDNA probe (Fig. 1*D*). TDAG51 mRNA transcripts of ~7 kb were detected in all human tissues examined, and the expression profile was similar to that of *GRP78*. The observation that TDAG51 and *GRP78* expression were most abundant in pancreas, an organ active in protein secretion and sensitive to ER stress (23), is consistent with the high level expression of two additional ER stress response genes, namely *Herp* (15) and *ORP150* (26).

Cellular Distribution of TDAG51—Subcellular fractionation experiments showed that TDAG51 was found predominantly in the cytoplasm, but not the nucleus, of untreated HUVEC (Fig. 4*A*). To elucidate the cytosolic localization of TDAG51, indirect immunofluorescence confocal microscopy was performed using anti-TDAG51 antibodies (Fig. 4, *B–E*). TDAG51 primarily localized in the cytoplasm of HUVEC in vesicles of two types: large vesicles found near the perinuclear region (Fig. 4*B*) and smaller vesicles at the periphery of the cell (Fig. 4*C*). Similar TDAG51 immunostaining was observed for HAEC, human aortic smooth muscle cells, and hepatocytes (data not shown). Co-localization studies in HUVEC using antibodies to TDAG51 and to specific cellular marker proteins, including membrin (Golgi), HSP60 (mitochondria), GRP78 (ER), H4A3 (lysosomes), catalase (peroxisomes), and focal adhesion kinase, revealed that TDAG51 associated with the large perinuclear vesicles co-localized with peroxisomes (Fig. 4*D*), whereas TDAG51 associated with the smaller vesicles co-localized with focal adhesion complexes (Fig. 4*E*). GRP78 also showed co-localization with TDAG51 in the larger perinuclear vesicles; however, membrin, HSP60, and H4A3 showed no co-localization with TDAG51. Treatment of HUVEC with homocysteine affected TDAG51 distribution (Fig. 4, *F–H*). A 30-min treatment of HUVEC with 1 mM homocysteine resulted in reduced density of the smaller peripheral TDAG51-positive vesicles, with the larger vesicles remaining perinuclear in distribution (Fig. 4*G*), compared with untreated controls (Fig. 4*F*). The typical distribution of TDAG51 positive vesicles returned after 24-h treatment; however, the intensity of TDAG51 staining appeared to increase in both small and large vesicles (Fig. 4*H*), a finding consistent with the immunoblot analysis. No specific immunostaining was observed when nonimmune goat IgG was used as the primary antibody (data not shown).

Overexpression of TDAG51 Causes Morphological Changes, Decreases Cell Adherence, and Promotes Detachment-mediated Programmed Cell Death—Previous studies have demonstrated that homocysteine induces PCD in HUVEC through activation of the UPR (18). In support of these findings, homocysteine induced a dose-dependent (50 μM to 10 mM) increase in PCD in HAEC, as measured by DNA fragmentation (Fig. 5*A*) and TUNEL staining (data not shown). As a positive control, tumor necrosis factor-α in the presence of actinomycin D also increased DNA fragmentation. However, cysteine, methionine, and homocystine did not promote PCD in HAEC.

Given that homocysteine induces the expression of TDAG51 and promotes PCD, we assessed the effect of TDAG51 overexpression on cell viability and integrity. Expression plasmids encoding GFP or a GFP-TDAG51 fusion protein were transiently transfected into cultured vascular endothelial cells. To verify expression of the recombinant proteins, immunoblot analysis was performed using antibodies specific to TDAG51 or GFP (Fig. 5*B*). HUVEC and HAEC (data not shown) transfected with the GFP-TDAG51 expression plasmid produced a fusion protein with an apparent molecular mass of 67 kDa, which was immunoreactive for both anti-TDAG51 and anti-GFP antibodies, a finding consistent with the predicted fusion between TDAG51 (40 kDa) and GFP (27 kDa). Cells transfected

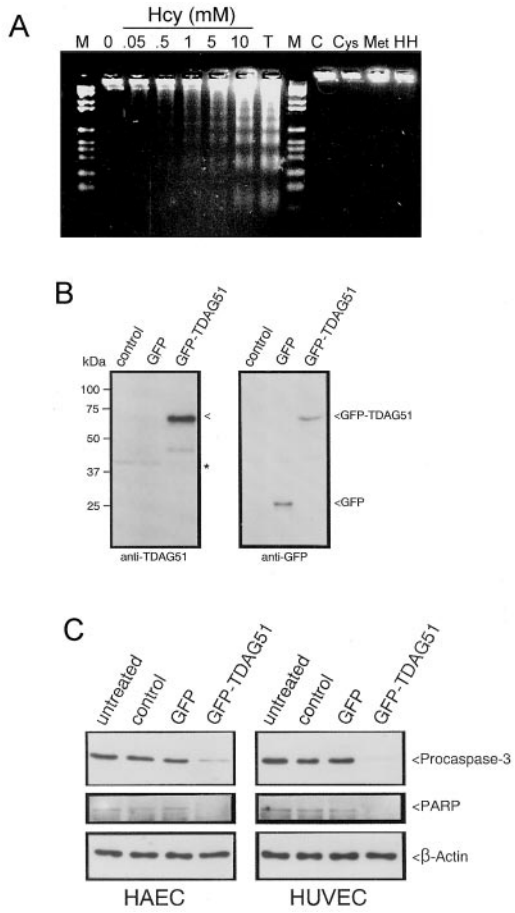

FIG. 5. **Induction of PCD by homocysteine or TDAG51 overexpression in vascular endothelial cells.** *A*, homocysteine induces PCD in HAEC. HAEC were cultured in the absence (*0* and *C*) or presence of 0.05–10 mM homocysteine (*Hcy*), 0.5 mM methionine (*Met*), 0.5 mM cysteine (*Cys*), or 0.5 mM homocystine (*HH*) for 24 h. As a positive control for PCD, HAEC were treated with tumor necrosis factor-α in the presence of actinomycin D (*T*). Following treatment, chromosomal DNA was isolated and separated on a 2% agarose gel, as described under "Experimental Procedures." *B*, expression of GFP or GFP-TDAG51 fusion protein in HUVEC. Total protein lysates (40 μg/lane) from cells transiently transfected for 24 h with transfection reagent alone (*control*) or transfection reagent containing 2 μg of the pEGFP (*GFP*) or pEGFP-TDAG51 (*GFP-TDAG51*) expression plasmids were subjected to immunoblot analysis using antibodies against GFP or TDAG51. The *arrowheads* indicate the migration position of GFP or GFP-TDAG51 fusion protein. The *asterisk* indicates the migration position of endogenous TDAG51. *C*, overexpression of GFP-TDAG51 fusion protein in HUVEC or HAEC activates caspase-3 and PARP. Total protein lysates from untreated cells (*untreated*) or cells transiently transfected for 24 h with transfection reagent alone (*control*) or transfection reagent containing 2 μg of the pEGFP (*GFP*) or pEGFP-TDAG51 (*GFP-TDAG51*) expression plasmids were subjected to immunoblot analysis using antibodies directed against procaspase-3 or PARP. To control for protein loading, immunoblots were reprobed with anti-β-actin antibodies.

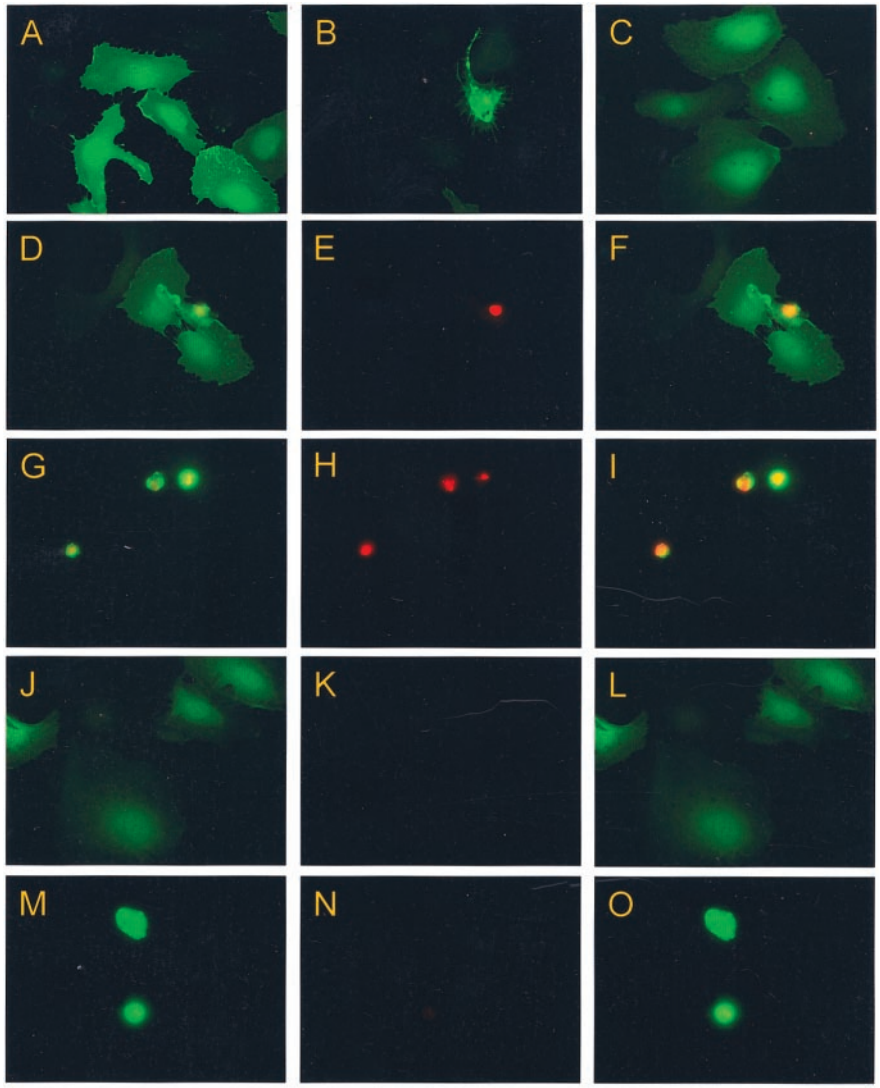

FIG. 6. **Overexpression of TDAG51 causes dramatic alterations in endothelial cell morphology and promotes detachment-mediated PCD.** HUVEC plated on gelatin-coated coverslips were transiently transfected with 2 μg of the pEGFP or pEGFP-TDAG51 expression plasmids, and cells showing nuclear DNA fragmentation were identified by TUNEL staining. *A* and *B*, GFP-TDAG51-overexpressing HUVEC, 12 or 24 h post-transfection, respectively. *C*, GFP-positive HUVEC, 24 h post-transfection. Also shown are adherent GFP-TDAG51-positive HUVEC (*D*) demonstrating TUNEL-positive staining (*E*), 12 h post-transfection. *F*, merged image of *D* and *E*. Nonadherent GFP-TDAG51 positive HUVEC (*G*) demonstrating TUNEL-positive staining (*H*), 24 h post-transfection, are shown. *I*, merged image of *G* and *H*. Adherent GFP positive HUVEC (*J*) demonstrating TUNEL-negative staining (*K*), 24 h post-transfection, are shown. *L*, merged image of *J* and *K*. *M–O*, pretreatment with ZVAD decreases TUNEL staining but does not prevent morphological changes and loss in adherence in HUVEC overexpressing GFP-TDAG51. Nonadherent GFP-TDAG51 positive HUVEC pretreated for 18 h with 20 μM ZVAD (*M*) demonstrating TUNEL-negative staining (*N*), 24 h post-transfection, are shown. *O*, merged image of *M* and *N*. Original magnification was ×630. Results are representative of four independent experiments.

with the GFP expression plasmid contained the expected 27-kDa GFP protein.

Overexpression of the GFP-TDAG51 fusion protein caused dramatic changes in cell morphology, including rounding up, membrane ruffling, and long pseudopodial extensions (Fig. 6, *A*, *B*, and *D*), compared with cells overexpressing GFP (Fig. 6*C*). Disruption of the actin cytoskeleton was also observed in the GFP-TDAG51-overexpressing cells (data not shown). Following these changes in cell morphology, there was clear evidence of PCD (Fig. 6, *E* and *F*), with a significant number of cells ($p < 0.001$) becoming detached from the tissue culture dishes in a dose- and time-dependent manner (Fig. 7*A*). Virtually all of the nonadherent cells expressing GFP-TDAG51 (Fig. 6*G*) were TUNEL-positive (Fig. 6, *H* and *I*) and corresponded to a significant increase in cell death ($p < 0.001$), as measured by the release of lactate dehydrogenase (Fig. 7*B*). Furthermore, GFP-TDAG51 overexpression induced the cleavage of both procaspase-3 and PARP in HUVEC and HAEC (Fig. 5*C*). In contrast, cells overexpressing GFP were morphologically normal (Fig. 6, *C* and *J*), remained adherent (Fig. 7*A*), and did not undergo PCD, as measured by TUNEL staining (Fig. 6, *K* and *L*, and Fig. 7*B*), caspase-3 activation, and PARP cleavage (Fig. 5*C*). Similar findings were observed in human aortic smooth muscle cells and macrophages overexpressing the GFP-TDAG51 fusion protein (data not shown). The observation of similar changes in cell morphology (data not shown) and increased detachment/cytotoxicity in cells overexpressing the native TDAG51 protein (Fig. 7*C*) suggests that these effects directly involve TDAG51 and are not due to acquired dominant properties of the fusion protein.

To determine whether the changes in cell morphology and adherence induced by TDAG51 were dependent on the activation of caspases, HUVEC were pretreated with the pancaspase inhibitor, ZVAD, prior to transient transfection with the GFP-TDAG51 expression plasmid (Fig. 6, *M–O*). ZVAD did not prevent the changes in either cell morphology or loss in cell adherence; however, it did inhibit TUNEL staining. These findings indicate that TDAG51-mediated changes in cell morphology and adherence are not dependent on caspase activation and suggest that TDAG51 promotes detachment-induced PCD (anoikis).

TDAG51 Expression Is Increased and Correlates with Programmed Cell Death in Atherosclerotic Lesions from apoE$^{-/-}$ Mice Having Diet-induced Hyperhomocysteinemia—Consistent with our previous findings (6), mice fed diets supplemented with methionine or homocysteine for 18 weeks became hyperhomocysteinemic and had significant increases in aortic root lesion size (Table I). To examine the effect of hyperhomocysteinemia on TDAG51 expression in atherosclerotic lesions, sections from the aortic root of apoE$^{-/-}$ mice fed control, high methionine, or high homocysteine were immunostained for TDAG51. In mice fed control diet, immunohistochemical stain-

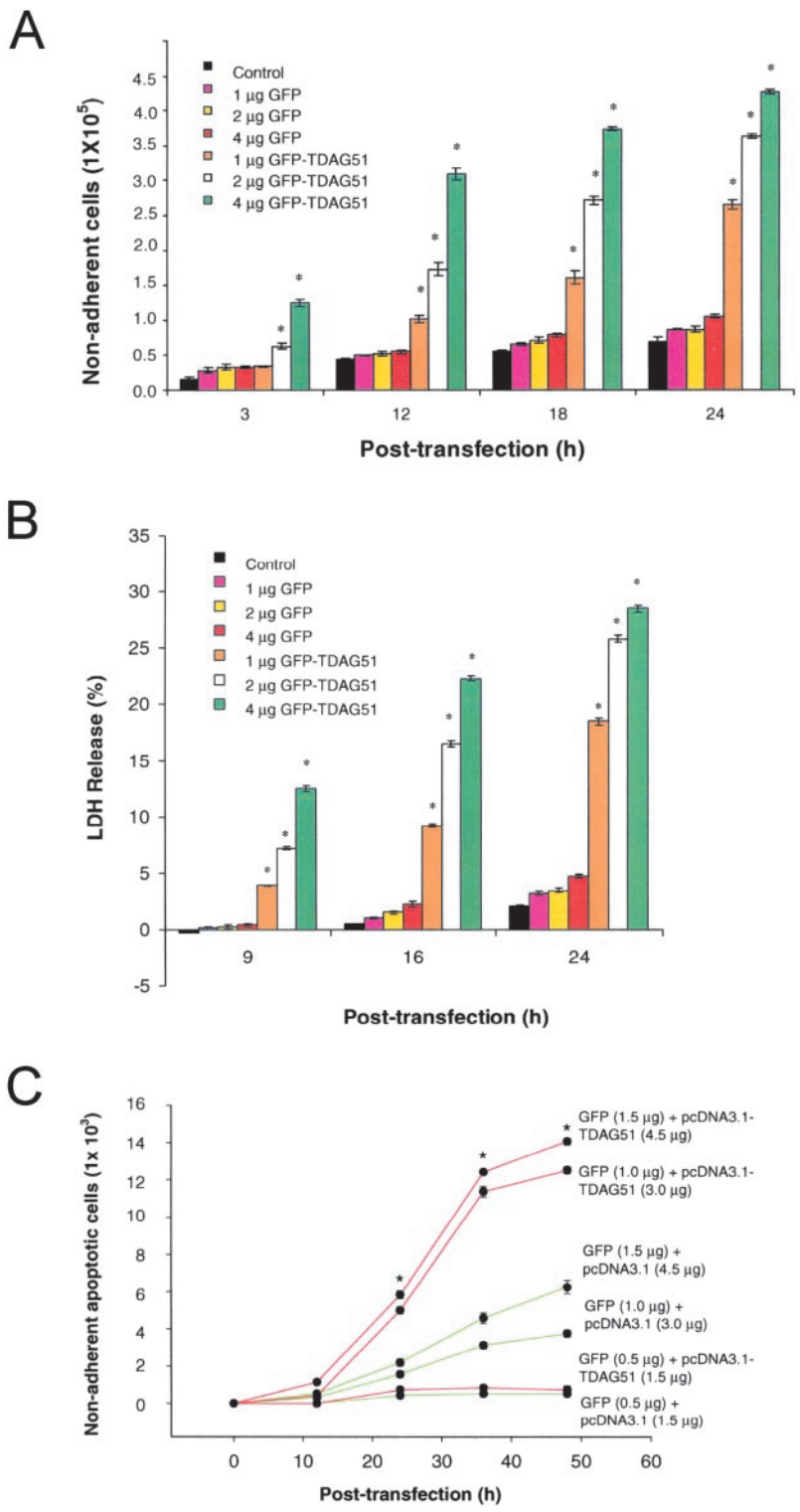

FIG. 7. **Overexpression of TDAG51 in endothelial cells decreases cell adherence and increases cell death in a dose- and time-dependent manner.** HUVEC (1×10^6) transiently transfected with transfection reagent (*control*) or transfection reagent containing increasing concentrations of the pEGFP (*GFP*) or pEGFP-TDAG51 (*GFP-TDAG51*) expression plasmids were grown for various time periods up to 24 h. *A*, identification of nonadherent GFP-positive cells in the medium, post-transfection. *B*, assessment of cell death by lactate dehydrogenase (*LDH*) release into the medium, post-transfection. *C*, overexpression of native TDAG51 in HUVEC. HUVEC (1.5×10^5) were co-transfected with the expression plasmids pEGFP (*GFP*) and either pcDNA3.1 or pcDNA3.1-TDAG51 for various time periods up to 48 h. Medium was collected, and nonadherent/apoptotic GFP-positive cells were subsequently identified and counted. Results are presented as the mean ± S.E. from three separate experiments. *, $p < 0.001$ *versus* vector control cells.

ing of the aortic wall showed that TDAG51 was confined to the atherosclerotic lesion (Fig. 8*A*). However, TDAG51 immunostaining was much more intense and widely distributed throughout the lesion and aortic wall of mice fed hyperhomocysteinemic diets (Fig. 8, *B* and *C*). Aortic root sections immunostained with nonimmune goat IgG as the primary antibody showed no detectable immunofluorescence signal within the aortic wall (Fig. 8*D*). Increased plasma homocysteine and aortic root lesion size were also observed in mice fed a high methionine diet for 4 weeks, compared with mice fed control diet (Table I). TDAG51 immunostaining was found predominantly within these early lesions but was increased in mice fed a high methionine diet (Fig. 8*F*), compared with mice fed the control diet (Fig. 8*E*).

To determine whether TDAG51 expression correlated with PCD, atherosclerotic lesions from mice fed control or hyperhomocysteinemic diets for 18 weeks (Fig. 9*A*) or 4 weeks (Fig. 9*B*) were immunostained for TDAG51 and assayed by the TUNEL method. Compared with mice fed control diet, TDAG51 expression and PCD were increased and co-localized to the necrotic core of lesions from mice fed high methionine or high homocysteine diet for 18 weeks. Immunocytochemical studies suggested

TABLE I
Plasma total homocysteine levels and atherosclerotic lesion size in apoE$^{-/-}$ mice fed control or hyperhomocysteinemic diets

Female apoE$^{-/-}$ mice at 6 weeks of age were fed the indicated diet for 4 or 18 weeks. Values are the mean ± S.E.

Group (*n*)	Plasma homocysteine,	Lesion size in aortic root,
	μmol/liter	*μm^2 × 10^3*
18 weeks		
Control (36)	9.46 ± 0.14	175.1 ± 10.4
High methionine (15)	53.6 ± 4.3[a]	281.1 ± 27.6[a]
High homocysteine (15)	51.4 ± 1.5[a]	266.1 ± 16.3[a]
4 weeks		
Control (8)	5.18 ± 0.14	7.9 ± 0.5
High methionine (8)	15.6 ± 2.4[a]	14.0 ± 3.7

[a] $p < 0.01$ versus control group.

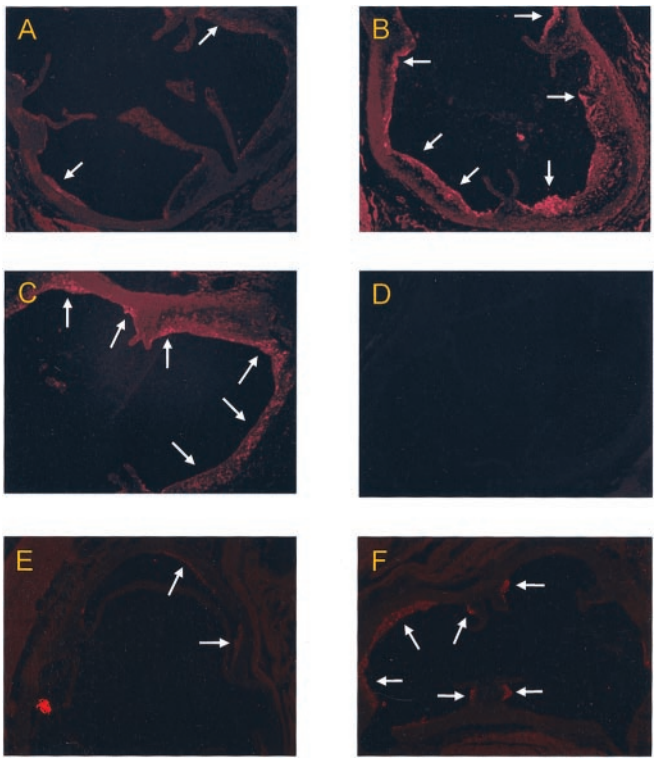

FIG. 8. **TDAG51 expression in the aortic root of apoE$^{-/-}$ mice fed control or hyperhomocysteinemic diets.** Shown is indirect immunofluorescence detection of TDAG51 in aortic root sections of apoE$^{-/-}$ mice fed control (*A*), high methionine (*B*), or high homocysteine (*C*) diet for 18 weeks. *D*, control section in which nonimmune goat IgG was used as the primary antibody. Shown is detection of TDAG51 in aortic root sections of apoE$^{-/-}$ mice fed control (*E*) or high methionine (*F*) diet for 4 weeks. Increased areas of TDAG51 immunostaining are indicated by the *arrows*. Original magnification was ×100.

that the majority of TDAG51/TUNEL-positive cells within the necrotic core were macrophages and smooth muscle cells (data not shown). However, endothelial cells positive for both TDAG51 and TUNEL were rarely observed in the aortic root wall. Although few TDAG51/TUNEL-positive cells were identified within the early lesions of mice fed control or high methionine diet for 4 weeks (Fig. 9*B*), there appeared to be more TUNEL-positive cells in the early lesions from hyperhomocysteinemic mice.

DISCUSSION

Recent studies have demonstrated that hyperhomocysteinemia accelerates the development of atherosclerosis (5, 6) and that homocysteine causes ER stress, leading to growth arrest and PCD in cultured vascular endothelial cells (10, 18, 19). Despite these findings, the proapoptotic factors implicated in

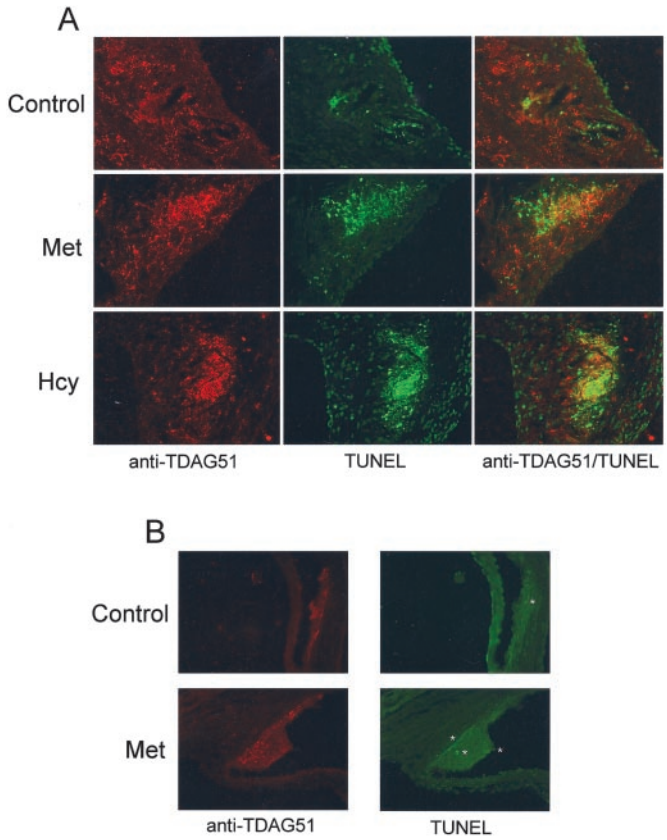

FIG. 9. **TDAG51 expression and PCD in atherosclerotic lesions from apoE$^{-/-}$ mice fed control or hyperhomocysteinemic diets.** *A*, identification of TDAG51 immunostaining and TUNEL-positive cells in sections from atherosclerotic lesions of apoE$^{-/-}$ mice fed control, high methionine (*Met*), or high homocysteine (*Hcy*) diet for 18 weeks. *B*, TDAG51 immunostaining and TUNEL-positive cells in sections from atherosclerotic lesions of apoE$^{-/-}$ mice fed control or high methionine (*Met*) diet for 4 weeks. TUNEL-positive cells are indicated by the *asterisks*. Original magnification was ×200.

this process and the *in vivo* relevance to atherogenesis have yet to be identified. We now provide evidence that TDAG51, a member of the pleckstrin homology-related domain family (20–22), is induced by homocysteine, promotes PCD, and contributes to the development of atherosclerosis in apoE$^{-/-}$ mice having diet-induced hyperhomocysteinemia. These findings are based on several lines of evidence presented here. First, homocysteine induces the expression of TDAG51 in cultured vascular endothelial cells in a time- and dose-dependent manner. Furthermore, the induction of TDAG51 by homocysteine involves ER stress and is dependent on eIF2α phosphorylation. Second, transient overexpression of TDAG51 causes dramatic changes in cell morphology, decreases cell adhesion, and promotes detachment-mediated PCD. Third, TDAG51 expression is increased in early and mature atherosclerotic lesions from apoE$^{-/-}$ mice fed hyperhomocysteinemic diets, compared with mice fed control diet. Fourth, a direct correlation between increased TDAG51 expression and PCD was observed in the atherosclerotic lesions from apoE$^{-/-}$ mice having diet-induced hyperhomocysteinemia. The additional observation that early and mature atherosclerotic lesions from apoE$^{-/-}$ mice fed hyperhomocysteinemic diets showed increased evidence of ER stress, as measured by GRP78/94 immunostaining,[2] suggests that TDAG51 contributes to the development of atherosclerosis through a mechanism involving ER stress.

TDAG51 is a member of a novel pleckstrin homology-related

[2] J. Zhou and R. C. Austin, manuscript in preparation

gene family that consists of *Ipl/Tssc* and *Tih* (20). Sequence analysis has revealed that TDAG51 contains a central motif resembling a pleckstrin homology domain and several distinctive C-terminal proline-glutamine and proline-histidine repeats, suggesting a role in transcriptional regulation and/or PCD (21, 22). Recent studies have now demonstrated that decreased expression of TDAG51 in metastatic melanoma correlates with increased resistance to PCD and that constitutive overexpression of TDAG51 increases PCD sensitivity and impairs melanoma cell proliferation (27). However, the precise mechanism by which TDAG51 mediates PCD is not known. Although TDAG51 has been shown *in vitro* to play critical roles in the up-regulation of *Fas* gene expression and activation-induced PCD of T cells (22), TDAG51$^{-/-}$ mice express normal levels of Fas with no impairment in T-cell PCD (28). Furthermore, TDAG51 fails to increase Fas expression and does not promote Fas-dependent PCD in rat H19-7 neuronal cells (21). Based on these reports, there is no clear evidence implicating TDAG51 in this Fas-dependent cell death pathway. However, given that overexpression of TDAG51 leads to dramatic alterations in cell shape and increases detachment of cells from their appropriate matrix, our findings support a mechanism involving detachment-mediated PCD or anoikis. Since caspase-mediated cytoskeletal/shape changes are a rather rapid process (29), the observation that TDAG51-induced shape changes are independent of caspase activation and occur prior to activation of the cell death program further supports a mechanism involving detachment-mediated PCD. Although the underlying mechanism by which TDAG51 overexpression induces detachment-mediated PCD is unknown, recent experiments have shown that expression of active integrin-linked kinase or Akt prevents anoikis, and cell detachment down-regulates survival functions of integrin-linked kinase (30–33). In addition, disruption of cell-extracellular matrix interaction also liberates Bfm from the cytoskeleton, which subsequently binds to and neutralizes the survival function of Bcl-2 (34). Because TDAG51 colocalizes with focal adhesion kinase and alters the actin cytoskeleton, it is conceivable that TDAG51 overexpression disrupts focal adhesion complex assembly and interrupts survival signaling from the extracellular matrix prior to activation of the cell death program.

In addition to its ability to decrease cell growth and promote PCD, TDAG51 has been reported to inhibit protein synthesis, possibly by interacting with cellular factors involved in the regulation of protein translation (35). It is well established that activation of the UPR by ER stress leads to decreased rates of protein synthesis (36), a process mediated by the ER-resident kinase, PERK (23, 25, 37). Once activated by ER stress signals, PERK phosphorylates Ser^{51} of eIF2α, thereby inhibiting cellular mRNA translation and inducing transcriptional activation of a wide range of ER stress-inducible genes, including *GRP78*, *GADD153*, and *TDAG51* (23). Given that homocysteine causes ER stress, the ability of homocysteine to increase TDAG51 expression, activate PERK (38, 39), and induce eIF2α phosphorylation (39) is not surprising.

Previous studies have proposed that acute clinical manifestations of atherosclerosis result from atherosclerotic lesion rupture, thereby triggering thrombus formation and vessel occlusion (40, 41). PCD has been well documented to occur in animal and human atherosclerotic lesions (42–44). The distribution of cell death is heterogeneous within the lesion, being more concentrated in regions containing a high density of macrophages and smooth muscle cells. Based on these findings, it has been suggested that PCD increases the risk of rupture by decreasing the stability of the atherosclerotic lesion. Furthermore, PCD enhances thrombogenicity by increasing the number of tissue factor-rich apoptotic microparticles within the atherosclerotic lesion (45). Given our findings that TDAG51 expression and PCD are increased and co-localize in the atherosclerotic lesions from apoE$^{-/-}$ mice having diet-induced hyperhomocysteinemia, TDAG51 could potentially alter lesion stability and/or thrombogenicity. Indeed, although a rare event in mice, we have documented spontaneous rupture of a coronary lesion in mice having diet-induced hyperhomocysteinemia (6). Further studies are, however, necessary to better define the prothrombotic effects of TDAG51.

Our findings clearly demonstrate that TDAG51 overexpression in culture vascular endothelial cells causes dramatic changes in cell morphology, decreases cell adhesion, and promotes PCD. However, very few TDAG51/TUNEL-positive endothelial cells were observed in early or mature atherosclerotic lesions from apoE$^{-/-}$ mice having diet-induced hyperhomocysteinemia. Because endothelial cells are increased in the circulation of patients with vascular disease following methionine load (46), it is possible that the majority of TDAG51/TUNEL-positive endothelial cells may have lost their adhesive properties and were shed into the circulation. This would be consistent with our finding that TDAG51 overexpression causes a loss in cell adhesion prior to PCD.

Although our studies implicate TDAG51 as an important proapoptotic factor that contributes to the development of atherosclerosis, additional cellular factors are likely to be involved. We and others have demonstrated that homocysteine induces the expression of *GADD153* (13–16), a basic region leucine zipper transcription factor that is markedly induced in response to a variety of cellular stresses (47). GADD153 correlates with ER stress-induced cell death (48), and overexpression of GADD153 sensitizes cells to ER stress by down-regulating Bcl-2 expression and enhancing oxidant injury (49). In addition, overexpression of GADD153 has been linked to the induction of PCD in 3T3 fibroblasts, keratinocytes, and HeLa cells (50). Further experimentation is needed to better elucidate the contributions of both TDAG51 and GADD153 to ER stress-induced PCD and in the development of atherosclerosis.

In summary, our findings support an important role for TDAG51 in promoting detachment-mediated PCD *in vitro* and *in vivo* and in contributing to the development of atherosclerosis in hyperhomocysteinemia. These findings should provide further insight into the molecular mechanisms leading to atherogenesis and provide opportunities for the development of therapeutic modalities useful in the treatment of this disease.

Acknowledgments—We thank Drs. Alana Majors, Henry Klamut, and Alistair Ingram for critical reading of this manuscript and Dr. Jaerang Rho for kindly providing the mouse *TDAG51* cDNA probe. We also acknowledge Dr. Donalyn Scheuner for making the homozygous A/A eIF2α mutant MEF available.

REFERENCES

1. Boushey, C. J., Beresford, S. A. A., Omenn, G. S., and Motulsky, A. G. (1995) *JAMA* (*J. Am. Med. Assoc.*) **274,** 1049–1057
2. Eikelboom, J. W., Lonn, E., Genest, J., Hankey, G., and Yusuf, S. (1999) *Ann. Intern. Med.* **131,** 363–375
3. Malinow, M. R., Bostom, A. G., and Krauss, R. M. (1999) *Circulation* **99,** 178–182
4. Welch, G. N., and Loscalzo, J. (1998) *N. Engl. J. Med.* **338,** 1042–1050
5. Hofmann, M. A., Lalla, E., Lu, Y., Gleason, M. R., Wolf, B. M., Tanji, N., Ferran, L. J., Kohl, B., Rao, V., Kisiel, W., Stern, D. M., and Schmidt, A. M. (2001) *J. Clin. Invest.* **107,** 675–683
6. Zhou, J., Møller, J., Danielsen, C. C., Bentzon, J., Ravn, H. B., Austin, R. C., and Falk, E. (2001) *Arterioscler. Thromb. Vasc. Biol.* **21,** 1470–1476
7. Starkebaum, G., and Harlan, J. M. (1986) *J. Clin. Invest.* **77,** 1370–1376
8. Jacobsen, D. W. (2000) *Arterioscler. Thromb. Vasc. Biol.* **20,** 1182–1184
9. Jacobsen, D. W. (2001) in *Homocysteine in Heath and Disease* (Carmel, R., and Jacobsen, D. W., eds) pp. 425–440, Cambridge University Press, Cambridge, UK
10. Outinen, P. A., Sood, S. K., Pfeifer, S. I., Pamidi, S., Podor, T. J., Li, J., Weitz, J. I., and Austin, R. C. (1999) *Blood* **94,** 959–967
11. Upchurch, G. R., Welch, G. N., Fabian, A. J., Freedman, J. E., Johnson, J. L., Keaney, J. F., and Loscalzo, J. (1997) *J. Biol. Chem.* **272,** 17012–17017

12. Jakubowski, H. (1997) *J. Biol. Chem.* **272,** 1935–1942
13. Outinen, P. A., Sood, S. K., Liaw, P. C. Y., Sarge, K. D., Maeda, N., Hirsh J., Ribau, J., Podor, T. J., Weitz, J. I., and Austin, R. C. (1998) *Biochem. J.* **332,** 213–221
14. Kokame, K., Kato, H., and Miyata, T. (1996) *J. Biol. Chem.* **271,** 29659–29665
15. Kokame, K., Agarwala, K. L., Kato, H., and Miyata, T. (2000) *J. Biol. Chem.* **275,** 32846–32853
16. Werstuck, G. H., Lentz, S. R., Dayal, S., Hossain, G. S., Sood, S. K., Shi, Y. Y., Zhou, J., Maeda, N., Krisans, S. K., Malinow, M. R., and Austin, R. C. (2001) *J. Clin. Invest.* **107,** 1263–1273
17. Cai, Y., Zhang, C., Nawa, T., Aso, T., Tanaka, M., Oshiro, S., Ichijo, H., and Kitajima, S. (2000) *Blood* **96,** 2140–2148
18. Zhang, C., Cai, Y., Adachi, M. T., Oshiro, S., Aso, T., Kaufman, R. J., and Kitajama, S. (2001) *J. Biol. Chem.* **276,** 35867–35874
19. Huang, R. F. S., Huang, S. M., Lin, B. S., Wei, J. S., and Liu, T.-Z. (2001) *Life Sci.* **68,** 2799–2811
20. Frank, D., Mendelsohn, C. L., Ciccone, E., Svensson, K., Ohlsson, R., and Tycko, B. (1999) *Mamm. Genome* **10,** 1150–1159
21. Gomes, I., Xiong, W., Miki, T., and Rosner, M. R. (1999) *J. Neurochem.* **73,** 612–622
22. Park, C. G., Lee, S. Y., Kandala, G., Lee, S. Y., and Choi, Y. (1996) *Immunity* **4,** 583–591
23. Scheuner, D., Song, B., McEwen, E., Liu, C., Laybutt, R., Gillespie, P., Saunders, T., Bonner-Weir, S., and Kaufman, R. J. (2001) *Mol. Cell.* **7,** 1165–1176
24. Reddy, P. H., Stockburger, E., Gillevet, P., and Tagle, D. A. (1997) *Genomics* **46,** 174–182
25. Harding, H. P., Novoa, I., Zhang, Y., Zeng, H., Wek, R., Schapira, M., and Ron, D. (2000) *Mol. Cell.* **6,** 1099–1108
26. Ikeda, J., Kaneda, S., Kuwabara, K., Ogawa, S., Kobayashi, T., Matsumoto, M., Yura, T., and Yanagi, H. (1997) *Biochem. Biophys. Res. Commun.* **230,** 94–99
27. Neef, R., Kuske, M. A., Pröls, E., and Johnson, J. P. (2002) *Cancer Res.* **62,** 5920–5929
28. Rho, J., Gong, S., Kim, N., and Choi, Y. (2001) *Mol. Cell. Biol.* **21,** 8365–8370
29. Kothakota, S., Azuma, T., Reinhard, C., Klippel, A., Tang, J., Chu, K., McGarry, T. J., Kirschner, M. W., Koths, K., Kwiatkowski, D. J., and Williams, L. T. (1997) *Science* **278,** 294–298
30. Frisch, S. M., and Screaton, R. A. (2001) *Curr. Opin. Cell Biol.* **13,** 555–562
31. Attwell, S., Roskelley, C., and Dedhar, S. (2000) *Oncogene* **19,** 3811–3815
32. Bachelder, R. E., Wendt, M. A., Fujita, N., Tsuruo, T., and Mercurio, A. M. (2001) *J. Biol. Chem.* **276,** 34702–34707
33. Fujio, Y., and Walsh, K. (1999) *J. Biol. Chem.* **274,** 16349–16354
34. Puthalakath, H., Villunger, A., O'Reilly, L. A., Beaumont, J. G., Coultas, L., Cheney, R. E., Huang, D. C. S., and Strasser, A. (2001) *Science* **293,** 1829–1832
35. Hinz, T., Flindt, S., Marx, A., Janssen, O., and Kabelitz, D. (2001) *Cell. Signalling* **13,** 345–352
36. Wong, W. L., Brostrom, M. A., Kuznetsov, G., Gmitter-Yellen, D., and Brostrom, C. O. (1993) *Biochem. J.* **289,** 71–79
37. Harding, H. P., Zhang, Y., and Ron, D. (1999) *Nature* **397,** 271–274
38. Nonaka, H., Tsujino, T., Watari, Y., Emoto, N., and Yokoyama, M. (2001) *Circulation* **104,** 1165–1170
39. Ma, K., Vattem, K. M., and Wek, R. C. (2002) *J. Biol. Chem.* **277,** 18728–18735
40. Fuster, V. (1994) *Circulation* **90,** 2126–2146
41. Lee, R. T., and Libby, P. (1997) *Arterioscler. Thromb. Vasc. Biol.* **17,** 1859–1867
42. Isner, J. M., Kearney, M., Bortman, S., and Passeri, J. (1995) *Circulation* **91,** 2703–2711
43. Kockx, M. M., Demeyer, G. R. Y., Muhring, J., Bult, H., Bultinck, J., and Herman, A. G. (1996) *Atherosclerosis* **120,** 115–124
44. Hegyi, L., Skepper, J. N., Cary, N. R., and Mitchison, M. J. (1996) *J. Pathol.* **180,** 423–442
45. Tedgui, A., and Mallat, Z. (2001) *Thromb. Haemost.* **86,** 420–426
46. Hladovec, J., Sommerova, Z., and Pisarikova, A. (1997) *Thromb. Res.* **88,** 361–364
47. Ron, D., and Habener, J. F. (1992) *Genes Dev.* **6,** 439–453
48. Zinszner, H., Kuroda, M., Wang, X. Z., Batchvarova, N., Lightfoot, R. T., Remotti, H., Stevens, J. L., and Ron, D. (1998) *Genes Dev.* **12,** 982–995
49. McCullough, K. D., Martindale, J. L., Klotz, L.-O., Aw, T.-Y., and Holbrook, N. J. (2001) *Mol. Cell. Biol.* **21,** 1249–1259
50. Maytin, E. V., Ubeda, M., Lin, J. C., and Habener, J. F. (2001) *Exp. Cell Res.* **267,** 193–204